Flash-Induced FTIR Difference Spectra of the Water Oxidizing Complex in Moderately Hydrated Photosystem II Core Films: Effect of Hydration Extent on S-State Transitions†

Takumi Noguchi*,‡ and Miwa Sugiura§

Biophysical Chemistry Laboratory, RIKEN, Wako, Saitama 351-0198, Japan, Institute of Materials Science, University of Tsukuba, Tsukuba, Ibaraki 305-8573, Japan, and Department of Applied Biological Chemistry, Faculty of Agriculture, Osaka Prefecture University, 1-1 Gakuen-cho, Sakai, Osaka, 599-8531 Japan

Received October 19, 2001; Revised Manuscript Received December 12, 2001

ABSTRACT: Differently hydrated films of photosystem II (PSII) core complexes from *Synechococcus elongatus* were prepared in a humidity-controlled infrared cell. The relative humidity was changed by a simple method of placing a different ratio of glycerol/water solution in the sealed cell. The extent of hydration of the PSII film was lowered as the glycerol ratio increased. FTIR difference spectra of the water oxidizing complex upon the first to sixth flashes were measured at 10 °C using these hydrated PSII films. The FTIR spectra (1800−1200 cm^{-1}) of the PSII films hydrated using 20% and 40% glycerol/water showed basically the same features as those of the core sample in solution [Noguchi, T., and Sugiura, M. (2001) *Biochemistry 40*, 1497−1502], and the prominent peaks exhibited clear period four oscillation patterns. These observations indicate that the S-state cycle properly functions in these hydrated samples. In the PSII films less hydrated, however, the efficiencies of S-state transitions decreased as the extent of hydration was lowered. This tendency was more significant in the $S_2 \rightarrow S_3$ and $S_3 \rightarrow S_0$ transitions than in the $S_1 \rightarrow S_2$ and $S_0 \rightarrow S_1$ transitions, indicating that the reactions or movements of water molecules are more strongly coupled with the former two transitions than the latter two. The implication of this observation was discussed in light of the water oxidizing mechanism especially in respect to the steps of substrate incorporation and proton release. Furthermore, in the OH stretching region (3800−3000 cm^{-1}) of the first-flash spectrum, a differential signal was observed at 3618/3585 cm^{-1}, which was previously found in the S_2/S_1 spectrum of a frozen sample at 250 K and assigned to the water vibrations [Noguchi, T., and Sugiura, M. (2000) *Biochemistry 39*, 10943−10949]. The fact that the signal appeared even in rather dehydrated PSII films at a physiological temperature (10 °C) supported the idea that this water is located in the close vicinity of the Mn cluster and directly involved in the water oxidizing reaction. The results also showed that moderate hydration of the PSII sample made the whole OH region measurable, escaping from absorption saturation by bulk water, and thus will be a useful technique to monitor the water reactions during the S-state cycle using FTIR spectroscopy.

In photosynthesis of plants and cyanobacteria, water is utilized as a terminal electron donor to reduce CO_2 for synthesis of starch. Oxidation of water is performed in the water oxidizing complex (WOC),[1] which resides on the electron donor side of photosystem II (PSII) (*1*, *2*). The structural core of WOC is the so-called Mn cluster, which consists of four Mn ions and one Ca ion. The structure of the Mn cluster has been studied using EXAFS (*3*−*5*) and EPR (*6*, *7*) spectroscopies, and various models in which the Mn ions are connected via μ-oxo bridges have been proposed, including the most popular structure of a dimer of di-μ-oxo dimer (*3*). On the other hand, recently the X-ray crystal structure of PSII at 3.8 Å resolution showed that the electron density fits well to a trimer−monomer structure (*8*). In the WOC, two water molecules are oxidized so that molecular oxygen and four protons are produced. This reaction proceeds through a light-driven cycle of five intermediates, S_0-S_4. The S_0, S_1, S_2, and S_3 states are relatively stable, and each state is advanced to the next state by single-flash turnover. The S_4 state is less stable and thermally relaxes to the S_0 state releasing molecular oxygen. The S_1 state is most dark stable, and hence dark-adapted PSII yields oxygen upon three flashes first and then every four flashes. The molecular mechanism of photosynthetic water oxidation is largely unknown, although various models have been proposed to date (*2*, *4*, *5*, *9*−*18*). The following questions have to be addressed: (i) What is the structure of the Mn cluster in each S-state intermediate? (ii) When do substrate water

† This work has been supported by a grant for the Bioarchitect Research Project of RIKEN given by the Ministry of Education, Culture, Sports, Science and Technology of Japan.

* To whom correspondence should be addressed. Phone: +81-298-53-5126. Fax: +81-298-55-7440. E-mail: tnoguchi@ims.tsukuba.ac.jp.

‡ RIKEN and University of Tsukuba.

§ Osaka Prefecture University.

[1] Abbreviations: CW, continuous wave; DM, *n*-dodecyl β-D-maltoside; ENDOR, electron nuclear double resonance; EPR, electron paramagnetic resonance; ESEEM, electron spin−echo envelope modulation; EXAFS, extended X-ray absorption fine structure; FTIR, Fourier transform infrared; IR, infrared; Mes, 2-(*N*-morpholino)ethanesulfonic acid; PSII, photosystem II; RH, relative humidity; WOC, water oxidizing complex.

10.1021/bi011954k CCC: $22.00
Published on Web 01/16/2002

molecules enter into the reaction cycle? (iii) Where is the binding site of substrate water in WOC? (iv) What are the structures of water intermediates in each S-state and when an O−O bond is formed? (v) What is the mechanism of proton release? (vi) How are amino acid residues and proteins involved in the reaction?

The questions ii, iii, and iv are concerned about substrate water, and addressing these questions is essential for understanding the water oxidizing mechanism. At the same time, however, there has been substantial difficulty in examining the reactions and structures of water because it is the solvent in the system as well. Most of the models assume that substrate water enters into the catalytic site during the $S_3 \rightarrow S_0$ transition coupled with O_2 evolution (*4*, *9*, *12*−*15*, *17*), while Hillier and Wydrzynski (*19*, *20*) predicted that water molecules enter during the $S_2 \rightarrow S_3$ and $S_3 \rightarrow S_0$ transitions from their results of $H_2{}^{18}O$ exchange rate detected by mass spectrometry. As for the binding site of substrate, a general view is that the two water molecules are bound to the Mn ions (*4*, *9*, *10*, *12*, *16*), but some models predict one of them is bound to the Ca ion (*13*, *14*, *18*). Experimentally, several attempts have been made to detect water molecules in WOC to date. The NMR relaxation rate of solvent protons, which is dependent on interaction with paramagnetic species, is enhanced by S-state changes, and this phenomenon was interpreted as due to rapid equilibrium between the protons of bulk water and those of Mn-coordinated water (*21*). Water binding to the Mn cluster was also suggested by CW EPR studies, in which small changes were observed in the S_2 multiline signal in $H_2{}^{17}O$ (*22*) and D_2O (*23*), being inconsistent with the reports of no change in D_2O (*24*, *25*). Britt (*2*) showed the presence of water or hydroxo ligands to Mn in both the S_1 and S_2 states by ESEEM of D_2O-exchanged PSII particles. Evans et al. (*26*) also observed interaction of D_2O with WOC in the S_2 state by ESEEM, in contrast to their previous study using $H_2{}^{17}O$ and D_2O-reconstituted PSII in which they could not obtain evidence of H_2O binding (*27*). In proton ENDOR studies, Kawamori et al. (*28*) and Fiege et al. (*29*) detected protons from water ligands to the Mn cluster, whereas Tang et al. (*30*) did not observe signals from un-ionized water or hydroxo ligands directly bound to the Mn cluster. Wydrzynski and co-workers (*19*, *20*, *31*, *32*) showed by mass spectrometric measurements that the rate of ^{18}O incorporation has biphasic kinetics in all S-states and thus substrate water is bound at two different metal sites. Recently, Cua et al. (*33*) measured resonance Raman spectra in the low-frequency region and found several bands sensitive to D_2O/H_2O exchange in the S_1 state. They suggested that the S_1 state of the Mn cluster contains at least two H_2O or OH^- ligands.

FTIR difference spectroscopy is a powerful method to study the structures and molecular interactions of cofactors and substrates in active sites of proteins and to monitor enzymatic reactions (*34*−*36*). This method has been applied to the research of photosynthetic water oxidation for several years (*37*−*54*). Spectra of WOC have been measured mostly on the first $S_1 \rightarrow S_2$ transition (*37*−*45*, *47*−*49*, *51*−*53*). Our analyses of the S_2/S_1 difference spectra in the mid-IR region of 1800−1000 cm^{-1} have revealed the structure of the protein moiety of WOC: the presence of carboxylate ligands and their interactions (*37*−*40*, *43*), the structure of a histidine ligand (*42*), changes in conformations of the polypeptide chains (*37*, *39*, *40*), and the structural coupling of a tyrosine residue with the Mn cluster (*41*). Zhang et al. (*47*) measured an $S_2Q_B^-/S_1Q_B$ spectrum using a rapid-scan time-resolved method at room temperature and showed striking similarities to the S_2/S_1 spectrum at cryogenic temperatures. Chu et al. (*48*, *49*, *51*−*53*) obtained S_2/S_1 spectra in the lower frequency region of 1000−350 cm^{-1} and assigned the 606/625 cm^{-1} bands to the Mn−O−Mn vibration by ^{18}O substitution (*51*). Chu et al. (*53*) further showed that the 606 cm^{-1} band shifted to 612 cm^{-1} in the D1−D170H mutant, indicating that D1−Asp170 is structurally coupled to the Mn−O−Mn structure. As for water in WOC, we have recently observed OH vibrations at 3618/3585 cm^{-1} in the S_2/S_1 spectrum, which were suggested to arise from substrate water, and showed that this water has a significantly asymmetric hydrogen-bonding structure (*45*). More recently, Hillier and Babcock (*54*) and we (*46*) have measured FTIR difference spectra of all the flash-induced S-state transitions ($S_1 \rightarrow S_2$, $S_2 \rightarrow S_3$, $S_3 \rightarrow S_0$, and $S_0 \rightarrow S_1$) and observed a period four oscillation in the signals. Thus, using the flash-induced FTIR difference technique, it became possible to study more details on the molecular mechanism of water oxidation through the S-state cycle.

One of the general methods to study the reaction of substrate in the catalytic mechanism of an enzyme is examining the effect of substrate concentration. In the case of WOC, this corresponds to changing the water content in a PSII sample. In this study, we have attempted this type of experiment by preparing PSII core films hydrated to different extents by developing a simple method to control the relative humidity in an IR cell using a glycerol/water solution. The effects on the S-state transitions in these hydrated PSII films were examined using flash-induced FTIR difference spectroscopy.

Another aim of this study is to establish a method for detecting the water OH region of FTIR difference spectra for all S-state transitions. The water OH bands have been obtained only in an S_2/S_1 spectrum using a PSII sample in frozen solution (250 K) (*45*). Also, only the weakly hydrogen-bonded OH region in 3800−3500 cm^{-1} was measurable, whereas the strongly hydrogen-bonded water bands in 3500−3000 cm^{-1} could not be detected because of absorption saturation due to bulk water (*45*). In the measurements of all S-state transitions, we used a PSII sample in liquid solution (10 °C) to attain efficient S-state transitions. Since liquid water has OH stretching bands in higher frequencies than ice water, even weakly hydrogen-bonded water bands were not detectable due to strong absorption of bulk water (Noguchi and Sugiura, unpublished). In this study, we have solved the above problem of water saturation by preparing moderately hydrated PSII films. We have found a good condition of hydration, which makes the whole OH region measurable while retaining a functional S-state cycle.

MATERIALS AND METHODS

Oxygen-evolving PSII core complexes from *Synechococcus elongatus*, in which the carboxyl terminus of the CP43 subunit was genetically histidine tagged, were purified using Ni^{2+}-affinity column chromatography as described by Sugiura and Inoue (*55*). The PSII core complexes were suspended in 10 mM Mes−NaOH (pH 6.0) containing 5 mM

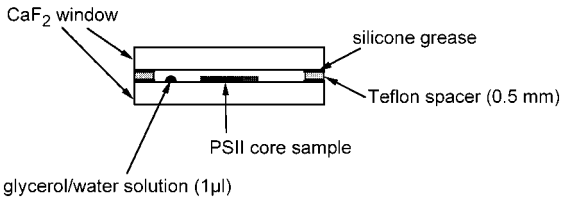

FIGURE 1: IR cell for a hydrated PSII film.

NaCl, 5 mM $CaCl_2$, and 0.06% DM and concentrated to about 4.5 mg of Chl/mL using Microcon-100 (Amicon). An aliquot of the core suspension (4 μL) was mixed with 1.0 μL of 100 mM potassium ferricyanide[2] and deposited on a CaF_2 window (25 mm ϕ × 3 mm) about 1 cm in diameter. The sample was then dried under N_2 gas flow for several minutes to generate a dry PSII film. A glycerol/water solution (1 μL) with different mixing ratio was placed on the window avoiding the sample area, and this window was covered by another CaF_2 window with a greased Teflon spacer (0.5 mm in thickness) to generate a sealed IR cell (Figure 1). The sample cell was fixed in a copper holder, in which the temperature was kept at 10 °C by circulating cold water. The sample was left at least for 1 h before flash-induced measurements to complete hydration of the PSII film. The process of hydration was monitored with an OH band of water (~3400 cm^{-1}) in FTIR spectra. The absorbance of the hydrated films was adjusted to 0.7−1.0 at the amide I peak at 1657 cm^{-1}.

Relative humidity (RH) was measured with a digital hygrometer, which was placed in a desiccator together with a glycerol/water solution with different mixing ratio.

FTIR spectra were measured on a Bruker IFS-66/S spectrophotometer equipped with an MCT detector (InfraRed D316/8). A Ge filter (OCLI, LO2584-9) was placed in front of the sample in an IR-beam path to block red light of a He−Ne laser from the interferometer. Another Ge filter was placed at the exit hole of the sample room to protect the MCT detector from scattering of laser pulses. Flash illumination was performed by nanosecond pulses from a frequency-doubled Q-switched Nd:YAG laser (Quanta-Ray GCR-130; 532 nm; ~7 ns fwhm). The pulse energy was ~10 mJ/(pulse cm^2) at the sample point. First, a dark-adapted PSII film was illuminated by two flashes to oxidize Y_D. After subsequent dark adaptation for 1 h, the sample was subjected to six consecutive flashes with a 10 s interval, and single-beam spectra (10 s scan) were measured before the first flash, between the flashes, and after the sixth flash. The sample was then dark adapted for 1 h again. The cycle of a train of six flashes and dark adaptation was repeated eight times, and the spectra were averaged. The 1 h period of dark adaptation is rationalized on the basis of the following values of S-state lifetimes. The lifetimes ($t_{1/2}$) of the S_2 and/or S_3 states of the PSII films under the present redox condition (in the presence of only ferricyanide) were estimated to be <20 min from the intensities of the S_2/S_1 signal of single-flash-induced FTIR difference spectra measured after 2 preflashes and subsequent dark relaxation for different periods. When the dark period is not long enough to relax the S_2 and S_3 states to the S_1 state, the S_2/S_1 intensity becomes smaller than that of the dark-adapted sample. Note that these lifetimes in the moderately hydrated PSII films are much larger than those in a solution sample estimated previously ($t_{1/2}$ < 3 min) (*46*). Furthermore, it was found that the S_0 state relaxes to S_1 with a lifetime ($t_{1/2}$) of about 80 s due to oxidation by ferricyanide, from the similar measurement using three flashes instead of two flashes. In this case, one preflash with subsequent dark adaptation was performed before the measurement to preoxidize Y_D. Thus, one-flash illumination in order to oxidize S_0 to S_1, which was adopted in our previous S-state measurements (*46*), was unnecessary. All spectra were measured with a resolution of 4 cm^{-1}. Simulation of the oscillation patterns and fitting of FTIR spectra were performed using the IGOR Pro program (Wavemetrics Inc.).

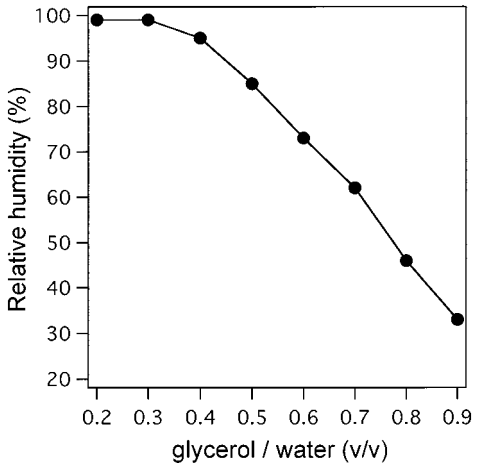

FIGURE 2: Relationship between the relative humidity by the presence of glycerol/water solution and its glycerol ratio obtained at 10 °C.

RESULTS AND DISCUSSION

The relative humidity in the IR cell was controlled by placing a small volume of glycerol/water solution in a sealed cell (Figure 1). Figure 2 presents the relationship between relative humidity and the mixing ratio (v/v) of glycerol/water solution at 10 °C. This plot clearly demonstrates that the relative humidity decreases as the glycerol ratio in the glycerol/water solution increases. A dry film of PSII core complexes from *S. elongatus* was hydrated under a desired humidity by changing the ratio of glycerol/water. Figure 3 shows the FTIR spectra of PSII core films hydrated under different relative humidities by the different ratios of glycerol/water solution. All of the spectra were normalized on the basis of the sharp bands in the 3000−2800 cm^{-1} region due to the CH stretching vibrations of methyl ($-CH_3$) and

[2] Previously, we showed that, in spinach PSII membranes, the presence of the ferrocyanide/ferricyanide (9:1) mixture prevents pre-oxidation of the non-heme iron and hence contamination of the S_2/S_1 difference spectrum with the non-heme iron signal (*39*, *67*). In the core complexes of cyanobacteria, however, this condition could not eliminate the non-heme iron contamination (*42*, *45*), probably because the midpoint potential of the non-heme iron is perturbed during preparation of the core complexes or it is originally different in cyanobacteria and in spinach. In this study as well as in our previous study of S-state spectra (*46*), we used only ferricyanide instead of the ferrocyanide/ferricyanide mixture. Judging from the intensity of the non-heme iron peak at 1100 cm^{-1} (not shown), the amount of the non-heme iron signal included in the first-flash spectrum was estimated to be about 15% of the total non-heme iron centers. Chu et al. (*48*) also reported that the non-heme iron signal made no significant contribution to their S_2/S_1 spectrum of the core complexes from spinach in the presence of only ferricyanide.

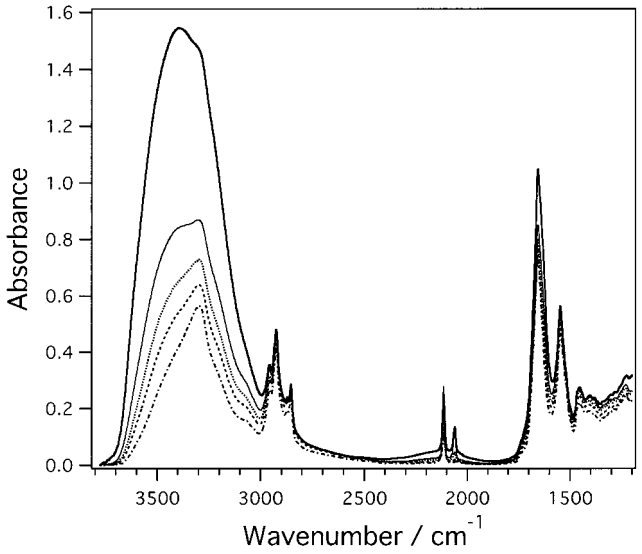

FIGURE 3: FTIR spectra of PSII core films from *S. elongatus* hydrated using 20% (99% RH; thick solid line), 40% (95% RH; thin solid line), 60% (73% RH; dotted line), and 80% (46% RH; dashed line) glycerol/water solutions and of a dry PSII film (dash−dotted line). All of the spectra were normalized to the spectrum of the dry film on the basis of the sharp CH stretching bands of methyl (−CH_3) and methylene (−CH_2−) groups in 3000−2800 cm^{-1}.

methylene (−CH_2−) groups. The peaks at 1657 and 1547 cm^{-1} are due to the amide I (C═O stretch) and amide II (N−H bend + C−N stretch) bands of polypeptide main chains. The H−O−H bending mode of water slightly contributes to the 1657 cm^{-1} band. The CN stretching band of ferricyanide, an exogenous electron acceptor, is observed at 2116 cm^{-1}. The ferrocyanide peak is also seen at 2062 cm^{-1},[3] which might be present in the sample simply as contamination or as a result of the redox reaction of ferricyanide with some PSII cofactor [Note that the extinction coefficient of the CN band is significantly larger in ferrocyanide than in ferricyanide (*56*).] IR absorption of water was observed as a broad O−H stretching band around 3400 cm^{-1}. In a dry film (no glycerol/water solution is placed in the cell), a broad feature is left around 3300 cm^{-1} (Figure 3, dash−dotted line), which arises mainly from the NH stretching vibrations of polypeptide main chains, with some contributions from the OH and NH stretching vibrations of amino acid residues and from the OH vibrations of detergent (DM) and internal water in the proteins. As the humidity in the IR cell increased, namely, the glycerol ratio (v/v) of the glycerol/water solution decreased from 80% (46% RH; dashed line) to 60% (73% RH; dotted line), 40% (95% RH; thin solid line), and 20% (99% RH; thick solid line), the water band around 3400 cm^{-1} became larger, indicating that the PSII film is more hydrated. It is noted that the hydration extent did not increase linearly relative to the RH value, because when the RH is close to 100%, the relationship

[3] Ferrocyanide in aqueous solution usually gives a CN stretching band at about 2040 cm^{-1}. However, in the presence of Ca^{2+} and PSII core complexes, the ferrocyanide band often shifts to about 2062 cm^{-1}. Flash-induced difference spectra also showed a ferrocyanide peak at 2062 cm^{-1} in addition to the normal 2040 cm^{-1} peak. This tendency varied from sample to sample. A similar upshift of a ferrocyanide peak was sometimes observed even in measurements using the PSII membranes from spinach. Although it is presumed that ferrocyanide makes some form of complex with Ca^{2+} and the PSII proteins, the precise reason for this frequency shift is unknown at present.

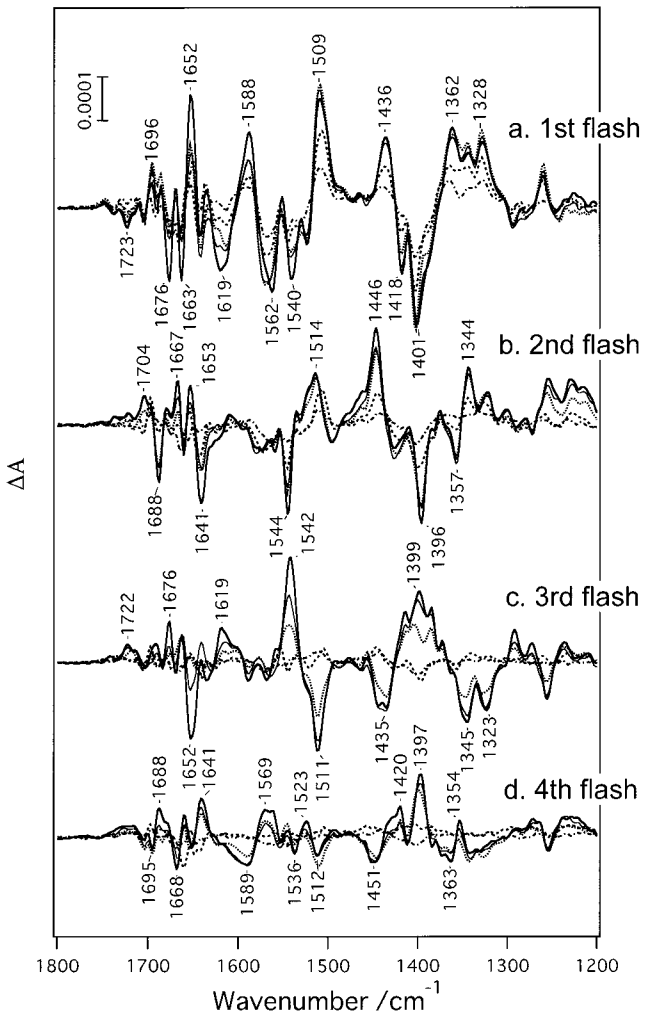

FIGURE 4: Flash-induced FTIR difference spectra (1800−1200 cm^{-1}) upon the first (a), second (b), third (c), and fourth (d) flash of PSII core films hydrated using 20% (thick solid line), 40% (thin solid line), 60% (dotted line), and 80% (dashed line) glycerol/water solutions and of a dry PSII film (dash−dotted line). Spectra were normalized using the same factors as those for the absorption spectra in Figure 3.

between the water content in the sample and RH does not hold linearity similarly to the case of the glycerol/water solution shown in Figure 2. When water without glycerol was placed in the IR cell (100% RH), the PSII sample absorbed too much water and became a liquidlike state, and hence the sample could not be held as a solid film any more.

Flash-induced FTIR difference spectra were measured using the above hydrated and dry PSII films. Figure 4 shows the obtained difference spectra upon the first to fourth flashes in the region of protein absorption (1800−1200 cm^{-1}). The spectra of the PSII films hydrated using 20% and 40% glycerol/water (thick and thin solid lines, respectively) exhibited basically the same spectral features as those of the previous spectra of a solution sample (*46*), indicating that these PSII films were hydrated enough to retain the functional S-state cycle. Previously, we showed that the first-, second-, third-, and fourth-flash spectra in the core complexes in solution virtually represent the S_2/S_1, S_3/S_2, S_0/S_3, and S_1/S_0 difference spectra, respectively, based on the fact that (i) all of the four spectra exhibited different band features, (ii) the spectra in the second S-state cycle (fifth-, sixth-, seventh-, and eighth-flash spectra) have the same features as the

corresponding spectra in the first S-state cycle (first-, second-, third-, and fourth-flash spectra, respectively), and (iii) prominent peaks showed clear period four oscillation patterns, which were simulated well with a 13% miss factor (*46*). Thus, the similarity of the spectra of the above PSII films to those of the solution sample also indicates that the first-, second-, third-, and fourth-flash spectra of these films (Figure 4, thick and thin solid lines) represent the S_2/S_1, S_3/S_2, S_0/S_3, and S_1/S_0 difference spectra, respectively. It should be noted that the previously reported distortion of spectra by superimposing broad bands of the COOH/COO^- changes (positive band around 1717 cm^{-1} and negative bands around 1567 and 1401 cm^{-1}) (*46*), which arise from nonspecific carboxylate groups of proteins by pH decrease during the S-state cycle, was much smaller and could be neglected in the present study. The main reason for this is that in this study one sample was subjected to only 50 flashes compared with about 240 flashes in the previous study (*46*). Hence, pH decrease was more prominent in the previous study. Also note that the bands of Mes buffer, which appear at about 1263(+)/1254(−)/1233(+) (+ and − indicate positive and negative peaks, respectively) upon protonation, contribute to the band features in 1300−1200 cm^{-1} in the second-, third-, and fourth-flash spectra. We simulated the oscillation patterns (up to the sixth flash) of the peak intensities for the spectra of the PSII film hydrated using 20% glycerol/water, using the peaks at 1344, 1357, 1401, 1418, 1436, 1446, 1509, and 1544 cm^{-1}, by the method described previously (*46*). All of the oscillation patterns were simulated well assuming 12% misses without COOH/COO^- correction (not shown).

In the above spectra of the PSII films hydrated using 20% and 40% glycerol/water (Figure 4, thick and thin solid lines, respectively), prominent peaks were observed in the regions of symmetric (1450−1300 cm^{-1}) and asymmetric (1600−1500 cm^{-1}) stretching modes of carboxylate (*39*, *40*, *43*), indicative of drastic structural changes of carboxylate groups during the S-state cycle. In addition, several strong peaks were observed in the region of amide I bands (1700−1600 cm^{-1}) arising from changes in protein conformation in WOC upon individual S-state transitions. The presence of amide I bands in difference spectra should be accompanied by amide II bands, which may superimpose the asymmetric COO^- bands around 1550 cm^{-1}. In fact, in the S_2/S_1 difference spectra of spinach PSII membranes, frequency shifts of some bands were observed in this region upon universal ^{15}N-labeling, strongly suggesting the presence of amide II bands in the spectra (*39*). It was noticed that although the first-flash spectrum of the film hydrated using 40% glycerol/water (Figure 4a, thin solid line) has almost the same intensity as that using 20% glycerol/water (Figure 4b, thick solid line) in the symmetric COO^- stretching region (1450−1300 cm^{-1}), bands in the amide I (1700−1600 cm^{-1}) and amide II (∼1550 cm^{-1}) regions showed slightly smaller intensities. The same tendency was observed in the other flash-induced spectra, for example, for the band at 1641 cm^{-1} in the second-flash spectra (Figure 4b, thick and thin solid lines) and for the 1652 and 1542 cm^{-1} bands in the third-flash spectra (Figure 4c, thick and thin solid lines). These observations indicate that the conformational changes of proteins in WOC are somehow restricted in less hydrated PSII complexes, even when they show functional S-state transitions. A similar phenomenon was previously observed in the P_{798}^+/P_{798} difference spectrum of a heliobacterium, in which drying the membrane sample dramatically decreased the bands in the amide I region (*57*).

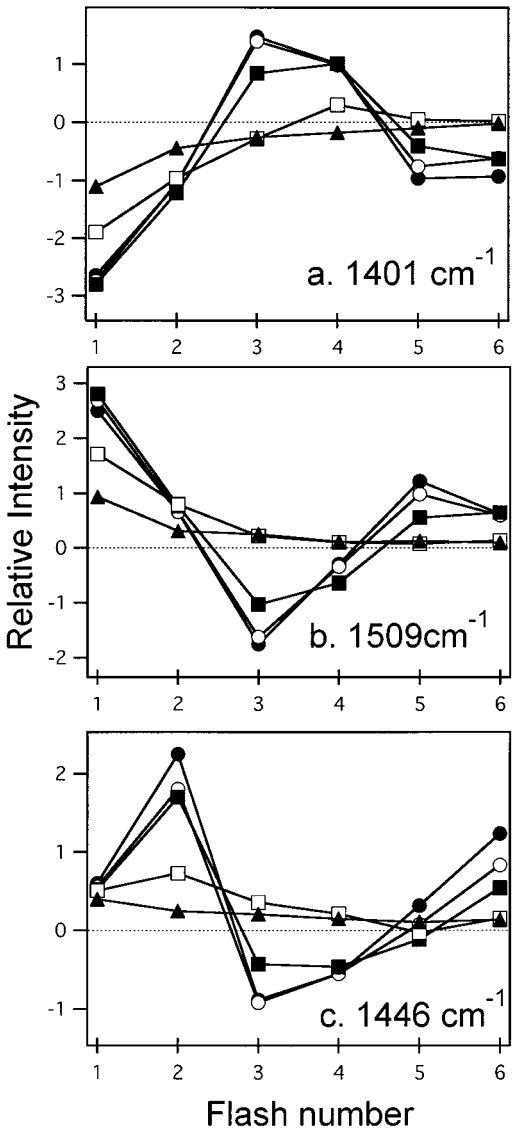

FIGURE 5: Flash-number dependent patterns of the relative intensities at 1401 (a), 1509 (b), and 1446 (c) cm^{-1} in the flash-induced FTIR spectra. The former two and the latter frequencies are the positions of the prominent peaks of the first- and second-flash spectra, respectively. The patterns are for the PSII films hydrated using 20% (filled circle), 40% (open circle), 60% (filled square). and 80% (open square) glycerol/water solutions and for the dry PSII film (filled triangle).

When PSII films were further dehydrated, more drastic changes were observed in flash-induced spectra (Figure 4). The PSII film hydrated using 60% glycerol/water (73% RH) clearly showed a smaller intensity in the third-flash spectrum (Figure 4c, dotted line). In the PSII film hydrated using 80% glycerol/water (46% RH) (Figure 4, dashed line) and the dry film (Figure 4, dash-dotted line), even the first-flash spectra became smaller, and after the third flash the spectra showed only weak features.

These spectral changes depending on the extent of hydration are better expressed in the flash-number dependent patterns (up to the sixth flash) of peak intensities shown in Figure 5. The relative intensities were plotted at 1401 (a) and 1509 (b) cm^{-1}, where prominent negative and positive

Table 1: Estimated Efficiencies of the S-State Transitions in the PSII Core Complexes Hydrated to Different Extents

glycerol/water (v/v %)[a]	relative humidity (%)	$S_1 \rightarrow S_2$	$S_2 \rightarrow S_3$	$S_3 \rightarrow S_0$	$S_0 \rightarrow S_1$
20	99	0.88 ± 0.02[b]	0.88 ± 0.02[b]	0.88 ± 0.02[b]	0.88 ± 0.02[b]
40	95	0.84 ± 0.01[e]	0.81 ± 0.02	0.77 ± 0.03	0.89 ± 0.05
60	73	0.84 ± 0.02[e]	0.67 ± 0.03	0.68 ± 0.03	0.76 ± 0.05
80	46	0.54 ± 0.01[e]	0.38 ± 0.03	0.31 ± 0.05	nd[d]
dry[c]		0.32 ± 0.01[e]	0.17 ± 0.02	0.06 ± 0.12	nd[d]

[a] The PSII core film was hydrated under the humidity by the presence of glycerol/water solution in a sealed IR cell (see text). [b] The efficiencies of the S-state transitions of the sample hydrated using 20% glycerol/water were estimated by simulation of the oscillation patterns of several prominent peaks using the method described in ref *46* assuming a single miss factor. The error was estimated from the standard deviation of the miss factor obtained in the fitting procedure. [c] The PSII film dried under N_2 gas flow for several minutes. [d] Not determined because of small spectral intensities. [e] The error was estimated from the standard deviations of the parameters obtained in the fitting procedure.

peaks, respectively, are present in the first-flash spectrum, and at 1446 cm^{-1} (c), where there is a prominent positive peak in the second-flash spectrum. In these patterns, a period four oscillation was clear for the PSII films hydrated using 20% (filled circle) and 40% (open circle) glycerol/water solutions. At 1401 and 1509 cm^{-1} the strong intensities at the first flash were restored at the fifth flash, and at 1446 cm^{-1} the strong positive intensities were observed at the second and sixth flashes. The oscillation pattern for the PSII film hydrated using 60% glycerol/water (filled square) was clearly damped compared with those for the more hydrated films. The PSII film hydrated using 80% glycerol/water (open square) did not show a oscillation pattern anymore, and only slight intensity was observed after the third flash. In the dry film, the first flash yeilded a relatively low intensity, which simply diminished as the flash number increased.

The efficiencies of the individual S-state transitions in the PSII films hydrated to different extents were estimated by fitting each flash-induced spectrum (Figure 4) using the spectra of the PSII film hydrated with 20% glycerol/water as standards. For simplicity, we first assume that the efficiencies of the S-state transitions in the PSII film hydrated using 20% glycerol/water are all unity (i.e., the first-, second-, third-, and fourth-flash spectra perfectly represent the S_2/S_1, S_3/S_2, S_0/S_3, and S_1/S_0 differences). The *n*th-flash ($n = 1-4$) spectra of the less hydrated PSII samples then can be expressed as linear combinations of these standard first−*n*th-flash spectra:

$$f_1(\nu) = a_1F_1(\nu)$$

$$f_2(\nu) = b_1F_1(\nu) + b_2F_2(\nu)$$

$$f_3(\nu) = c_1F_1(\nu) + c_2F_2(\nu) + c_3F_3(\nu)$$

$$f_4(\nu) = d_1F_1(\nu) + d_2F_2(\nu) + d_3F_3(\nu) + d_4F_4(\nu)$$

where $F_1(\nu)-F_4(\nu)$ represent the standard first−fourth-flash spectra of the PSII film hydrated using 20% glycerol/water (Figure 4, thick solid lines), $f_1(\nu)-f_4(\nu)$ represent the first−fourth-flash spectra of the other less hydrated PSII films (Figure 4), and a_1, b_1, b_2, c_1-c_3, and d_1-d_4 are the coefficients in linear combinations. The efficiencies of the $S_1 \rightarrow S_2$, $S_2 \rightarrow S_3$, $S_3 \rightarrow S_0$, and $S_0 \rightarrow S_1$ transitions can be calculated as a_1, b_2/a_1, c_3/b_2, and d_4/c_3, respectively. In the real case, however, efficiencies even in a fully hydrated PSII sample is slightly lower than unity due to misses, and those were estimated to be 0.88 (12% misses) for the film hydrated using 20% glycerol/water (see above). Thus, the efficiencies of the S-state transitions of the less hydrated samples can be obtained by multiplying the above values by 0.88 (i.e., $0.88a_1$, $0.88b_2/a_1$, $0.88c_3/b_2$, and $0.88d_4/c_3$ for $S_1 \rightarrow S_2$, $S_2 \rightarrow S_3$, $S_3 \rightarrow S_0$, and $S_0 \rightarrow S_1$, respectively).

We obtained the above coefficients in linear combinations by simple least-squares fitting of the spectra in the region of 1600−1200 cm^{-1}. The amide I region in 1700−1600 cm^{-1} was excluded for fitting, because of the strong hydration effect as mentioned above. It should be noted that, in the above equations, tighter constraints could be placed on the coefficients; the coefficients can be expressed using four independent parameters of the efficiencies of the individual S-state transitions. This should be the case if the sample is completely homogeneous. However, such assumption did not yield a satisfactory result in fitting of the spectra. This suggests that the PSII films are rather heterogeneous; it is considered, for instance, that the surface of the film is more hydrated than the inside.

The efficiencies of the individual S-state transitions of each PSII sample estimated using the above method are summarized in Table 1. It is seen that the efficiency values were lowered as the PSII films became less hydrated. This tendency was more significant in the $S_2 \rightarrow S_3$ and $S_3 \rightarrow S_0$ transitions than the $S_1 \rightarrow S_2$ and $S_0 \rightarrow S_1$ transitions. In the PSII film hydrated using 40% glycerol/water, the efficiencies of the $S_2 \rightarrow S_3$ and $S_3 \rightarrow S_0$ transitions (0.77−0.81) slightly decreased from the values using 20% glycerol/water (0.88), whereas those of the $S_1 \rightarrow S_2$ and $S_0 \rightarrow S_1$ transitions (0.84−0.89) were basically preserved. Also, in the film hydrated using 60% glycerol/water, the efficiencies of the $S_2 \rightarrow S_3$ and $S_3 \rightarrow S_0$ transitions were 0.67−0.68, in comparison with the efficiencies of 0.84 and 0.76 of the $S_1 \rightarrow S_2$ and $S_0 \rightarrow S_1$ transitions, respectively. Furthermore, in the film hydrated using 80% glycerol/water and the dry film, the $S_2 \rightarrow S_3$ and $S_3 \rightarrow S_0$ efficiencies largely decreased to 0.31−0.38 and 0.06−0.17, respectively, whereas the $S_1 \rightarrow S_2$ efficiencies were 0.54 and 0.32, respectively (the $S_0 \rightarrow S_1$ efficiencies in these films could not be estimated properly because of the weak features in the fourth-flash spectra).

The above observations that the $S_2 \rightarrow S_3$ and $S_3 \rightarrow S_0$ transitions are more susceptible to dehydration than the $S_1 \rightarrow S_2$ and $S_0 \rightarrow S_1$ transitions indicate that the reactions or movements of water molecules in WOC are more strongly coupled in the former two transitions compared with the latter two. The possible mechanisms are inferred as follows. (1) Substrate water molecules enter into the catalytic site of WOC in the $S_2 \rightarrow S_3$ and $S_3 \rightarrow S_0$ transitions. This idea is in agreement with the recent proposal by Hillier and Wydrzyn-

ski (*19*, *20*) based on the measurements of the $H_2{}^{18}O$ exchange rates that substrate water may enter the catalytic sequence during the $S_2 \rightarrow S_3$ and $S_3 \rightarrow S_0$ transitions. Also, this idea is basically consistent with the general view that substrate water is incorporated into the Mn cluster during the $S_3 \rightarrow S_0$ transition coupled with O_2 evolution (*4*, *9*, *12*−*15*, *17*). (2) Proton transfer mediating water molecules takes place in the $S_2 \rightarrow S_3$ and $S_3 \rightarrow S_0$ transitions. It is reasonable to think that proton transfer pathways coupled to water oxidation consist of both protonatable amino acid residues and water molecules. In fact, proton transfer pathways including water molecules are proposed in the acceptor side of bacterial reaction center (*58*, *59*) and cytochrome *c* oxidase (*60*) from the X-ray crystal structures. A consensus has not been reached yet on which transitions are coupled to proton release from substrate water, because of different patterns of proton release over the S-state transitions depending on materials and pH (*61*−*63*). Also, it has been proposed that there are a few different proton transfer pathways depending on the S-state transitions (*10*, *13*, *16*). Thus, it is possible that the $S_2 \rightarrow S_3$ and $S_3 \rightarrow S_0$ transitions use a proton transfer pathway different from that of the other transitions. This view is consistent with the idea by Brudvig and co-workers (*13*) that the concerted proton abstraction by Y_Z (*2*, *12*) takes place only in the $S_2 \rightarrow S_3$ and $S_3 \rightarrow S_4$ transitions and another pathway is used in other transitions. (3) Water molecules are significantly rearranged in WOC coupled to the reactions in the $S_2 \rightarrow S_3$ and $S_3 \rightarrow S_0$ transitions. Movements of water molecules will change the hydrogen bond network and dielectric environment in WOC and, thus, can be an important factor in the molecular mechanism of water oxidation. (4) Water is necessary to maintain the proper structure of WOC through hydrogen-bonding networks. The $S_2 \rightarrow S_3$ and $S_3 \rightarrow S_0$ transitions can be more susceptible to structural perturbation by dehydration. In fact, it has been known that these transitions are more susceptible to various modifications of WOC. The $S_2 \rightarrow S_3$ transition is blocked by Ca^{2+} depletion and Cl^- depletion (reviewed in refs *1* and *2*), and the $S_3 \rightarrow S_0$ rate is slowed during preparation of PSII membranes from thylakoid (*64*) and in the absence of the 33 kDa extrinsic protein (*65*).

The phenomenon of higher susceptibility of the $S_2 \rightarrow S_3$ and $S_3 \rightarrow S_0$ transitions to hydration extent may be caused by the mixed factors of above mechanisms. The present observations are also consistent with the activation energies E_A of individual transitions reported by Renger and co-workers (reviewed in refs 9 and 10). The E_A values for the $S_0 \rightarrow S_1$ and $S_1 \rightarrow S_2$ transitions are comparatively small, while E_A increases by a factor of 3 for the $S_2 \rightarrow S_3$ transition. In the $S_3 \rightarrow S_0$ transition, the E_A value changes at the characteristic temperature (ϑ_c), and at temperatures lower than ϑ_c (in the thermophilic bacterium *Synechococcus vulcanus*, which may be comparable to *S. elongatus*, ϑ_c was estimated to be 16 °C; the temperature used in this study was 10 °C), E_A was even higher than that for the $S_2 \rightarrow S_3$ transition. Since the extent of conformational changes of proteins revealed in the intensities of the amide I bands in the FTIR different spectra were more or less similar among the four S-state transitions (Figure 4, thick solid lines), rearrangements of water molecules and protons could be dominant reasons for higher E_A values in the $S_2 \rightarrow S_3$ and $S_3 \rightarrow S_0$ transitions. Similarly, our results may be related to the slower rates of the $S_2 \rightarrow S_3$ and $S_3 \rightarrow S_0$ transitions than the $S_1 \rightarrow S_2$ and $S_0 \rightarrow S_1$ transitions (*64*, *66*).

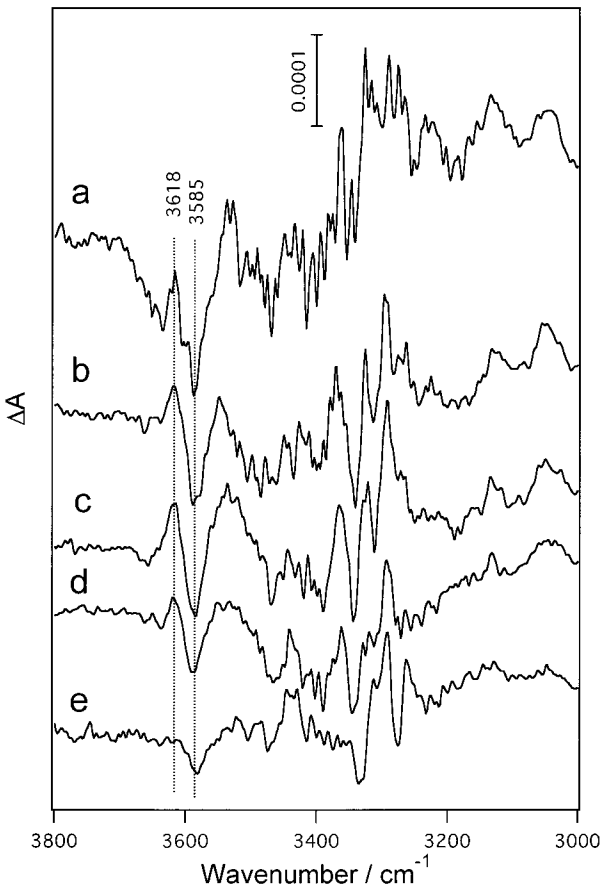

FIGURE 6: OH stretching region of the first-flash-induced FTIR difference spectra of the PSII films hydrated using 20% (a), 40% (b), 60% (c), and 80% (d) glycerol/water solutions and of the dry PSII film (e).

The result that all of the S-state transitions are more or less affected by dehydration (Table 1) is reasonable because all of the reactions in WOC should be coupled to water in some way. Alternatively, however, the result might reflect retardation of the rate of Y_Z oxidation by P_{680}, which should be coupled to the proton transfer either in the protein matrix or toward the lumen (*2*, *12*). Although we cannot argue the latter possibility any further at present, it may be interesting to investigate the dehydration effect on Y_Z oxidation in relevance to the hydrogen/proton abstraction model by Y_Z as a mechanism of proton release from substrate water (*2*, *12*).

Figure 6 shows the OH stretching region (3800−3000 cm^{-1}) of the first-flash spectra of the PSII films hydrated to different extents. A differential signal at 3618/3585 cm^{-1} was observed in all of the samples. Its intensity was smaller in the less hydrated PSII samples (Figure 6d,e), being consistent with the lower $S_1 \rightarrow S_2$ efficiencies. We previously observed the same signal in the S_2/S_1 spectrum of the PSII core complexes in solution measured at 250 K (*45*). The signal was assigned to the OH stretching bands of water coupled to the $S_1 \rightarrow S_2$ transition using $H_2{}^{18}O$ and D_2O substitution (*45*). The presence of this water signal in rather dehydrated PSII samples and the observation that the signal decreased proportionally to the $S_1 \rightarrow S_2$ efficiency support the idea that the observed water is not bulk water but present

in the close vicinity of the Mn cluster possibly as a substrate. In addition, observation of this water signal at 10 °C, not only in the frozen sample at 250 K, indicates that the structural change of this water molecule takes place as a physiological reaction.

The spectrum in the OH stretching region for the PSII film hydrated using 20% glycerol/water (Figure 6a) was rather noisy because of strong water absorption (Figure 3, solid line). In contrast, the less hydrated PSII samples (Figure 6b−e) showed a much smaller noise level in the whole OH region. Since the PSII film moderately hydrated using 40% glycerol/water exhibited almost fully functional S-state cycle (Table 1), this hydration condition would be appropriate for FTIR measurements of the water region for all of the S-state transitions. Several bands were observed in the 3500−3000 cm^{-1} region (Figure 6). Strongly hydrogen-bonded OH vibrations of water would be included in this feature, but various OH and NH vibrations of amino acid side chains and polypeptide backbones should also contribute to this spectral region. Further studies of isotope substitution are necessary for identifying water bands and precise assignments in this region. The water region spectra for other S-state transitions and the results of $H_2{}^{18}O$ and D_2O substitutions will be reported elsewhere.

REFERENCES

1. Debus, R. J. (1992) *Biochim. Biophys. Acta 1102*, 269−352.
2. Britt, R. D. (1996) in *Oxygenic Photosynthesis: The Light Reactions* (Ort, D. R., and Yocum, C. F., Eds.) pp 137−164, Kluwer, Dordrecht, The Netherlands.
3. Yachandra, V. K., DeRose, V. J., Latimer, M. J., Mukerji, I., Sauer, K., and Klein, M. P. (1993) *Science 260*, 675−679.
4. Yachandra, V. K., Sauer, K., and Klein, M. P. (1996) *Chem. Rev. 96*, 2927−2950.
5. Robblee, J. H., Roehl, M. C., and Yachandra, V. K. (2001) *Biochim. Biophys. Acta 1503*, 7−23.
6. Peloquin, J. M., Campbell, K. A., Randall, D. W., Evanchik, M. A., Pecoraro, V. L., Armstrong, W. H., and Britt, R. D. (2000) *J. Am. Chem. Soc. 122*, 10926−10942.
7. Zheng, M., and Dismukes, G. C. (1996) *Inorg. Chem. 35*, 3307−3319.
8. Zouni, A., Witt, H. T., Kern, J., Fromme, P., Krauss, N., Saenger, W., and Orth, P. (2001) *Nature 409*, 739−743.
9. Renger, G. (1997) *Physiol. Plant. 100*, 824−841.
10. Renger, G. (2001) *Biochim. Biophys. Acta 1503*, 210−228.
11. Rüttinger, W., and Dismukes, G. C. (1997) *Chem. Rev. 97*, 1−24.
12. Tommos, C., and Babcock, G. T. (1998) *Acc. Chem. Res. 31*, 18−25.
13. Vrettos, J. S., Limburg, J., and Brudvig, G. W. (2001) *Biochim. Biophys. Acta 1503*, 229−245.
14. Pecoraro, V. L., Baldwin, M. J., Caudle, M. T., Hsieh, W.-Y., and Law, N. A. (1998) *Pure Appl. Chem. 70*, 925−929.
15. Siegbahn, P. E. M., and Crabtree, R. H. (1999) *J. Am. Chem. Soc. 121*, 117−127.
16. Haumann, M., and Junge, W. (1999) *Biochim. Biophys. Acta 1411*, 86−91.
17. Nugent, J. H. A., Rich, A. M., and Evans, M. C. W. (2001) *Biochim. Biophys. Acta 1503*, 138−146.
18. Kuzek, D., and Pace, R. J. (2001) *Biochim. Biophys. Acta 1503*, 123−137.
19. Hillier, W., and Wydrzynski, T. (2000) *Biochemistry 39*, 4399−4405.
20. Hillier, W., and Wydrzynski, T. (2001) *Biochim. Biophys. Acta 1503*, 197−209.
21. Sharp, R. R. (1992) in *Manganese Redox Enzymes* (Pecoraro, V. L., Ed.) pp 177−196, VCH Publishers, New York.
22. Hansson, Ö., Andréasson, L.-E., and Vänngard, T. (1986) *FEBS Lett. 195*, 151−154.
23. Nugent, J. H. A. (1987) *Biochim. Biophys. Acta 893*, 184−189.
24. Yachandra, V. K., Guiles, R. D., Sauer, K., and Klein, M. P. (1986) *Biochim. Biophys. Acta 850*, 333−342.
25. Haddy, A., Aasa, R., and Andréasson, L.-E. (1989) *Biochemistry 28*, 6954−6959.
26. Evans, M. C. W., Rich, A. M., and Nugent, J. H. A. (2000) *FEBS Lett. 477*, 113−117.
27. Turconi, S., MacLachlan, D. J., Bratt, P. J., Nugent, J. H. A., and Evans, M. C. W. (1997) *Biochemistry 36*, 879−885.
28. Kawamori, A., Inui, T., Ono, T., and Inoue, Y. (1989) *FEBS Lett. 254*, 219−224.
29. Fiege, R., Zweygart, W., Bittl, R., Adir, N., Renger, G., and Lubitz, W. (1996) *Photosynth. Res. 48*, 227−237.
30. Tang, X.-S., Sivaraja, M., and Dismukes, G. C. (1993) *J. Am. Chem. Soc. 115*, 2382−2389.
31. Messinger, J., Badger, M., and Wydrzynski, T. (1995) *Proc. Natl. Acad. Sci. U.S.A. 92*, 3209−3213.
32. Hillier, W., Messinger, J., and Wydrzynski, T. (1998) *Biochemistry 37*, 16908−16914.
33. Cua, A., Stewart, D. H., Reifler, M. J., Brudvig, G. W., and Bocian, D. F. (2000) *J. Am. Chem. Soc. 122*, 2069−2077.
34. Mäntele, W. G. (1995) in *Anoxygenic Photosynthetic Bacteria* (Blankenship, R. E., Madigan, M. T., and Bauer, C. E., Eds.) pp 627−647, Kluwer, Dordrecht, The Netherlands.
35. Nabedryk, E. (1996) in *Infrared Spectroscopy of Biomolecules* (Mantsch, H. H., and Chapman, D., Eds.) pp 39−81, Wiley-Liss, New York.
36. Siebert, F. (1993) in *Biomolecular Spectroscopy* (Clark, R. J. H, and Hester, R. E., Eds.) Part A, pp 1−54, John Wiley & Sons, Chichester.
37. Noguchi, T., Ono, T., and Inoue, Y. (1992) *Biochemistry 31*, 5953−5956.
38. Noguchi, T., Ono, T., and Inoue, Y. (1993) *Biochim. Biophys. Acta 1143*, 333−336.
39. Noguchi, T., Ono, T., and Inoue, Y. (1995) *Biochim. Biophys. Acta 1228*, 189−200.
40. Noguchi, T., Ono, T., and Inoue, Y. (1995) *Biochim. Biophys. Acta 1232*, 59−66.
41. Noguchi, T., Inoue, Y., and Tang, X.-S. (1997) *Biochemistry 36*, 14705−14711.
42. Noguchi, T., Inoue, Y., and Tang, X.-S. (1999) *Biochemistry 38*, 10187−10195.
43. Noguchi, T., Sugiura, M., and Inoue, Y. (1999) in *Fourier Transform Spectroscopy* (Itoh, K., and Tasumi, M., Eds.) pp 459−460, Waseda University Press, Tokyo, Japan.
44. Onoda, K., Mino, H., Inoue, Y., and Noguchi, T. (2000) *Photosynth. Res. 63*, 47−57.
45. Noguchi, T., and Sugiura, M. (2000) *Biochemistry 39*, 10943−10949.
46. Noguchi, T., and Sugiura, M. (2001) *Biochemistry 40*, 1497−1502.
47. Zhang, H., Fischer, G., and Wydrzynski, T. (1998) *Biochemistry 37*, 5511−5517.
48. Chu, H.-A., Gardner, M. T., O'Brien, J. P., and Babcock, G. T. (1999) *Biochemistry 38*, 4533−4541.
49. Chu, H.-A., Hillier, W., Law, N. A., and Babcock, G. T (2000) *Biochim. Biophys. Acta 1503*, 69−82.
50. Chu, H.-A., Hillier, W., Law, N. A., Sackett, H., Haymond, S., and Babcock, G. T. (2000) *Biochim. Biophys. Acta 1459*, 528−532.
51. Chu, H.-A., Sackett, H., and Babcock, G. T. (2000) *Biochemistry 39*, 14371−14376.
52. Chu, H.-A., Gardner, M. T., Hillier, W., and Babcock, G. T. (2001) *Photosynth. Res. 66*, 57−63.
53. Chu, H.-A., Debus, R. J., and Babcock, G. T. (2001) *Biochemistry 40*, 2312−2316.
54. Hillier W., and Babcock, G. T. (2001) *Biochemistry 40*, 1503−1509.
55. Sugiura, M., and Inoue, Y. (1999) *Plant Cell Physiol. 40*, 1219−1231.
56. Jones, L. H. (1963) *Inorg. Chem. 2*, 777−780.
57. Noguchi, T., Fukami, Y., Oh-oka, H., and Inoue, Y. (1997) *Biochemistry 36*, 12329−12336.

58. Abresch, E. C., Paddock, M. L., Stowell, M. H. B., McPhillips, T. M., Axelrod, H. L., Soltis, S. M., Rees, D. C., Okamura, M. Y., and Feher, G. (1998) *Photosynth. Res. 55*, 119−125.
59. Fritzsch, G., Kampmann, L., Kapaun, G., and Michel, H. (1998) *Photosynth. Res. 55*, 127−132.
60. Tsukihara, T., Aoyama, H., Yamashita, E., Tomizaki, T., Yamaguchi, H., Shinzawa-Itoh, K., Nakashima, R., Yaono, R., and Yoshikawa, S. (1996) *Science 272*, 1136−1144.
61. Haumann, M., and Junge, W. (1996) in *Oxygenic Photosynthesis: The Light Reactions* (Ort, D. R., and Yocum, C. F., Eds.) pp 165−192, Kluwer, Dordrecht, The Netherlands.
62. Rappaport, F., and Lavergne, J. (2001) *Biochim. Biophys. Acta 1503*, 246−259.
63. Schlodder, E., and Witt, H. T. (1999) *J. Biol. Chem. 274*, 30387−30392.
64. Razeghifard, M. R., and Pace, R. J. (1997) *Biochim. Biophys. Acta 1322*, 141−150.
65. Razeghifard, M. R., Wydrzynski, T., Pace, R. J., and Burnap, R. L. (1997) *Biochemistry 36*, 14474−14478.
66. Babcock, G. T., Blankenship, R. E., and Sauer, K. (1976) *FEBS Lett. 61*, 286−289.
67. Noguchi, T., and Inoue, Y. (1995) *J. Biochem. 118*, 9−12.

BI011954K